Isomerization dynamics of a novel cis/trans-only merocyanine

ChemPhotoChem

Research Article
doi.org/10.1002/cptc.202300327

Chemistry Europe
European Chemical Societies Publishing

www.chemphotochem.org

Isomerization dynamics of a novel *cis/trans*-only merocyanine

Nadine Blaise[+],[a] James A. Green[+],[a] Carlos Benitez-Martin,[b] Christoph Kaiser,[a, c] Markus Braun,[a] Jonas M. Schaible,[a] Joakim Andréasson,[b] Irene Burghardt,*[a] and Josef Wachtveitl*[a]

Merocyanines (MC) usually adopt ring opened zwitterionic structures that are interconvertible with their ring-closed spiropyran photoisomers. By methylating the phenolate oxygen, and thereby blocking the ring-closure reaction, a *cis/trans*-only MC photoswitch was obtained, yielding a perfect candidate for a detailed examination of the *cis/trans* isomerization mechanism for this class of compounds. This photoswitch displays outstanding properties including excellent photoreaction quantum yields and photoswitching turnovers. Due to the central polymethine bridge of MC, in principle eight *cis* (C)/*trans*/(T) isomers are possible. Density Functional Theory (DFT) calculations revealed the CCT and TTT-isomers of the studied compound as most stable *cis* and *trans* ground state isomers, respectively. UV/vis transient absorption studies combined with conical intersection computations with the complete active space self-consistent field (CASSCF) method show that both *trans/cis*- and *cis/trans*-photoisomerizations are initiated by a rotation of the central doubled bond fragment. A hot ground state species is then formed, which undergoes a second isomerization. Thus, the *cis/trans* reaction proceeds via a CCT-CTT-TTT sequence and the reverse reaction via TTT-TCT-CCT.

Introduction

Photoswitches are popular candidates for diverse applications ranging from optoelectronics[1,2] and photocontrol of biological structures[3,4] to dye-sensitized solar cells.[5] Given their photochemical attributes, their photoisomers can be interconverted by external stimuli such as light, temperature, or both. In contrast to the most prominent azobenzene[6,7] *cis/trans* photoswitch, numerous representatives adopt a cyclization photoisomerization reaction, such as diarylethenes,[8] fulgimides[9] and spiropyrans.[10–12] Regarding their photoinduced change of molecular properties, spiropyrans are outstanding since the non-polar ring-closed spiropyran (SP) structure is converted into a ring-open zwitterionic merocyanine form (MC). Due to its planarity, the latter contains a strongly delocalized π-electron system, and consequently absorbs in the visible wavelength range. The ring-open structure has the property of a *push-pull* system – in particular when an electron-withdrawing group, such as -NO_2 is attached to the phenolic moiety (Scheme 1). In addition to photoinduced ring-closure, the MC-isomers undergo *cis/trans*-isomerizations, similar to azobenzenes,[13–16] fulgides[17,18] and hydrazones.[19,20] Ernsting *et al.* established that the formation of different MC isomers is based on the partial double bond character of the central methine linkage.[21] As a result of the three central bonds, there are $2^3 = 8$ different isomers, where *cis* (C) and *trans* (T) define the molecular geometry of the individual bonds. Typically, only the structures with a central *trans* geometry (hereafter *transoid*) represent stable MC isomers. In contrast, the configurations with a central *cis* geometry (hereafter *cisoid*) exhibit higher ground state energies due to internal steric hindrance and are therefore unstable. While SP→MC photoreactions have been extensively

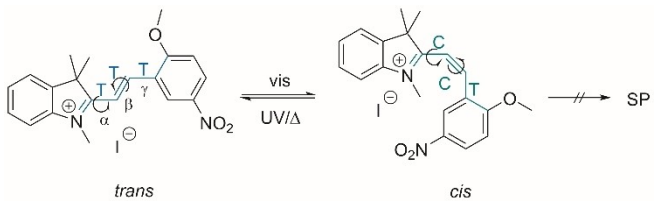

Scheme 1. Photoinduced and thermal isomerization between the TTT (*trans*) and CCT (*cis*) isomer of the studied MC derivative including the counter ion iodide. The crossed-out arrow indicates the absence of spiropyran (SP) formation, resulting from the methylation of the phenolate oxygen.

[a] *N. Blaise,[+] Dr. J. A. Green,[+] Dr. C. Kaiser, Dr. M. Braun, J. M. Schaible, Prof. I. Burghardt, Prof. J. Wachtveitl*
Institute of Physical and Theoretical Chemistry
Goethe University Frankfurt
Max-von-Laue-Straße 7, 60438 Frankfurt am Main
E-mail: wveitl@theochem.uni-frankfurt.de
burghardt@chemie.uni-frankfurt.de

[b] *Dr. C. Benitez-Martin, Prof. J. Andréasson*
Department of Chemistry and Chemical Engineering, Chemistry and Biochemistry
Chalmers University of Technology
SE-41296 Göteborg, Sweden

[c] *Dr. C. Kaiser*
Current address: AMOLF
Science Park 104
1098 XG Amsterdam, The Netherlands

[+] *These authors contributed equally to this work.*

Supporting information for this article is available on the WWW under https://doi.org/10.1002/cptc.202300327

studied,[22–25] less is known about the *cis*/*trans* isomerization mechanisms for the merocyanine form.

This is due in part to the large number of possible isomers in the ground and excited states, as well as possible environmental influences on the sample under investigation.

Our compound **2MeMC** differs drastically from the typical MC derivatives studied so far. While in past studies TTT (*trans-trans-trans*) and TTC (*trans-trans-cis*) represented the most stable configurations,[22,26] our compound exhibits a stable CCT isomer in addition to TTT. In some low temperature studies, TTC has been shown to be the most stable isomer in merocyanine compounds without alkylation of the phenolic oxygen and TTT the next most stable, while in this work with alkylation we observe the opposite stability.[27,28] This observation is explained by the methylation of the phenolate oxygen, which efficiently blocks the ring closing reaction to yield the SP isomer and results in a *cis*/*trans*-only photoswitch (Scheme 1). Thus, **2MeMC** is the perfect candidate for a detailed examination of the *cis*/*trans* isomerization mechanism for SP/MC photoswitches. **2MeMC** was previously investigated using steady-state UV/vis and NMR spectroscopy by Fleming *et al.*[29] In the present work, we expand the scope to include the ultrafast excited state dynamics of **2MeMC** using fs-transient absorption spectroscopy in protic and aprotic solvents to shed light on the *cis*/*trans* isomerization mechanism and the solvent influence on this important class of compounds. The experimental results are complemented with theoretical calculations by means of Density Functional Theory (DFT) and the Complete Active Space Self-Consistent Field (CASSCF) method. By combining quantum chemical calculations and time-resolved spectroscopy, we were able to elucidate the isomerization of **2MeMC** and provide information about the MC isomers involved.

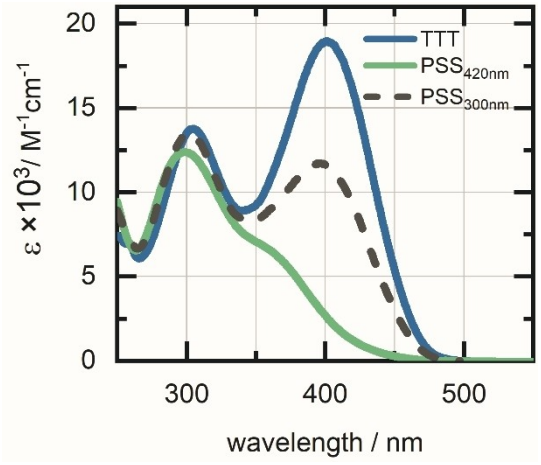

Figure 1. Absorption spectra of TTT (blue) and PSS_{420nm} (CCT, light green)-isomers of **2MeMC** in EtOH at room temperature and the PSS_{300nm} (dashed line) obtained upon exposure to 300 nm, scaled to the extinction coefficient ε.

Table 1. Photophysical properties of **2MeMC** in EtOH, MeCN and H_2O/EtOH (1:1). Quantum yields Φ of the TTT→CCT and the CCT→TTT photoreaction, composition of photostationary states (PSS) accumulated during irradiation with 420 nm or 300 nm, rate constants k for the thermal CCT→TTT isomerization at 25 °C.

solvent	EtOH	MeCN	H_2O/EtOH
$\Phi_{TTT\rightarrow CCT}$	62%	59%	68%
$\Phi_{CCT\rightarrow TTT}$	20%	46%	18%
PSS_{300nm}[a]	61%	48%	53%
PSS_{420nm}[b]	87%	75%	84%
$k_{25\,°C}/s^{-1}$	$6.9\cdot10^{-4}$	$5.8\cdot10^{-4}$	$3.0\cdot10^{-4}$

[a] formed TTT after 300 nm exposure. [b] turned TTT after photoconversion with 420 nm.

Results and Discussion

Thermal and photoinduced reactions

Typically, open MC isomers exhibit a dominant absorption band in the visible wavelength range, whereas the herein investigated **2MeMC** absorbs mainly in the UV range. This hypsochromic shift is associated with the methylation of the phenolate oxygen. Note the similarity to the absorption spectrum of a protonated merocyanine isomer (typically referred to as MCH). The stationary absorption spectrum of the stable TTT consists of two bands (Figure 1, blue). The dominant band of the TTT isomer is centered around 400 nm and exhibits an extinction coefficient $\varepsilon_{(400nm)}$ of ~19000 $M^{-1}cm^{-1}$ in EtOH. As in the previous study by Fleming *et al.*[29] (SI, Figure S14), it is assumed that this spectrum corresponds to 100% TTT. The absorption spectrum after exposure to light at 420 nm (PSS_{420nm}) displays a maximum at 300 nm with a distinct shoulder at 360 nm and an $\varepsilon_{(300nm)}$ of ~13000 $M^{-1}cm^{-1}$ (Figure 1, light green). This band corresponds to ~87% CCT, indicating residual TTT (Table 1) as a result of thermal relaxation CCT → TTT that prevents quantitative formation of CCT. However, this spectrum will be referred to as CCT.

In order to investigate the photophysical properties of **2MeMC**, wavelengths of 300 nm and 420 nm were used to excite the *cis*- and *trans*-isomer, respectively. At thermal equilibrium, the sample adopts its thermally stable TTT state. After exposure of TTT to 420 nm light its unique absorption band at 400 nm almost completely decays corresponding to a turnover ~84% (see determination in SI).

Since the absorption band of CCT has an additional shoulder around 360 nm it is also excited with light at 420 nm, as complete conversion of TTT is not possible. UV irradiation causes a joint excitation of both isomers, which does not fully restore the low-energy absorption band of TTT. This leads to a photostationary state (PSS_{300nm}) of 61% TTT in EtOH, and 48% in MeCN and 53% in H_2O/EtOH (Table 1). The associated TTT→CCT photoreaction quantum yields (QYs) indicate little or no influence of the solvent on this process (QYs of 62%, 59%, and 68% for EtOH, MeCN, and H_2O/EtOH, respectively, Table 1). The reverse photoreaction CCT→TTT shows a more pronounced solvent dependence, since quantum yields of 20%, 18% and 46% were determined in EtOH, H_2O/EtOH and MeCN, respectively. This could be related to the geometry of the CCT and

simultaneously to the proticity of EtOH and H_2O. Detailed information about the determination of QYs is described in the supplementary information. (SI).

Although the compound shows some photodegradation over multiple switching cycles (Figure S1), it still stands out for its efficient switching, manifested by isomerization quantum yields tenfold higher compared to the typical MC photoreaction.[30,31] Note that the photostability is improved in H_2O/EtOH (Figure S1), due to interactions of H_2O with the isomers leading to stabilization of the sample.[32] The activation energy (see Figure S3) for the thermal relaxation at 25 °C is 61 kJ/mol in EtOH, a similar value of 63 kJ/mol in MeCN, but exhibits a significantly higher value of 78 kJ/mol in H_2O/EtOH.

The rate constants of the thermal isomerization from CCT to TTT are comparable in MeCN and EtOH (Figure S2). The difference in activation energy is due to the fact that CCT is stabilized by water,[32,33] as evidenced by the highest value in the H_2O/EtOH mixture. In contrast to zwitterionic merocyanines, **2MeMC** showed no hydrolysis reaction in H_2O/EtOH at temperatures below 45 °C (Figure S2). Only above 45 °C an initial hydrolysis could be observed after about 30 min. The presence of an additional methyl group and thus an increase of the electron density in the system seems to significantly increase the stability of **2MeMC** and thus shows a stronger resistance to water.

The MC form is fluorescent, which allows for differentiation of various MC derivatives.[26,34] Therefore, the fluorescence properties of both isomers of **2MeMC** were investigated. In order to measure the fluorescence of the TTT isomer, an excitation wavelength of 400 nm was used. The broad and red-shifted emission spectrum of this configuration is centered at about 550 nm (Figure 2, blue spectra). The emission spectrum of the CCT after excitation at 300 nm, on the other hand, is narrower and localized at about 360 nm. Exemplarily, only the fluorescence in EtOH is shown because the fluorescence spectra do not change significantly in the different solvents (Figure S2).

Ultrafast photoinduced dynamics

In order to investigate the photodynamics of the individual photoisomers, ultrafast time-resolved measurements were performed. The photoisomerization of TTT→CCT was performed with a central excitation wavelength of 420 nm. To re-accumulate the TTT after excitation, the sample was back-illuminated with 300 nm during the measurement. For the reverse reaction CCT→TTT, an excitation wavelength of 300 nm was used and the back-exposure was performed with 420 nm. The analysis of the transient data was performed with the evaluation program OPTIMUS[35] where a global lifetime analysis was applied (more details in SI).

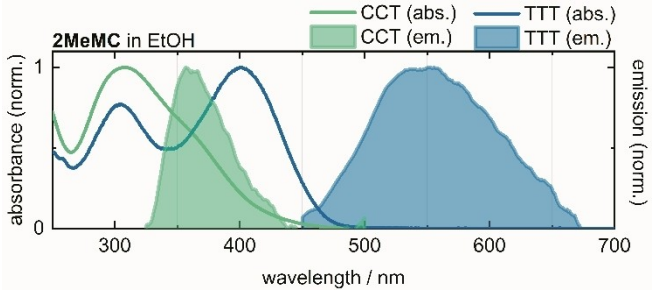

Figure 2. Absorption (solid line) and fluorescence spectrum (filled spectra) in EtOH of TTT (blue) and CCT (light green) **2MeMC**. The Raman peak at 450 nm was excised.

TTT→CCT photoisomerization

The transient data (Figure 3) of the TTT→CCT isomerization exhibits three dominant contributions – two positive excited state absorption (ESA) bands at 400 nm (Figure S4) and 470 nm and two negative signatures that can be assigned to the instantaneous bleach of the ground state absorption band (ground state bleach, GSB) at 400 nm and a stimulated emission (SE) band around 570 nm. All four contributions are directly present after excitation of **2MeMC**.

Four lifetimes were required to fit the data appropriately. Regardless of the solvent, the decay-associated spectra (DAS, Figure 3b, d) show similar contributions. The first lifetime describes an ultrafast decay of the positive contributions within <1 ps, as shown by the positive amplitudes at 400 nm and 500 nm (DAS, blue spectra). A positive signature at 400 nm is dominated by the bleach band and is therefore only seen in the DAS or lifetime-density map LDM (Figure S4). The positive contributions and the SE signature finally decay simultaneously with the second lifetime τ_2 (DAS, yellow spectra) and therefore belong to the same excited state (DAS, yellow spectra).

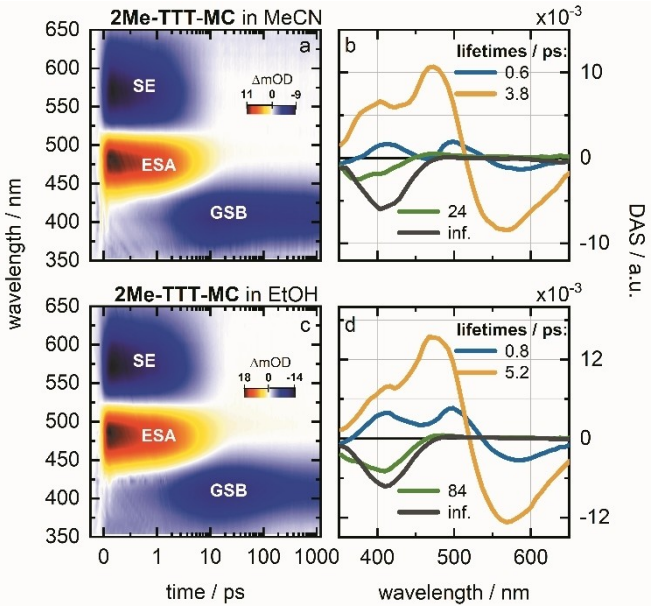

Figure 3. Transient absorption data of **2Me**-TTT-**MC** in MeCN (a and b) and EtOH (c and d) after excitation with 420 nm and corresponding decay-associated spectra (DAS), respectively. The negative absorption difference signals represent stimulated emissions (light and dark blue, SE) or ground-state bleaching (GSB) and the positive difference signals (yellow up to dark red) are associated with excited state absorption (ESA).

Spectrally, the SE band (525–650 nm) resembles the fluorescence of TTT (Figure 2), which describes the decay of the S_1 state according to Kasha's rule. After leaving the lowest excited state via a conical intersection (CoIn), a hot ground state S_0* is populated, which is accompanied by a less stable hot ground state isomer TCT. Starting from this *cisoid* form, the ground state barrier to the photoproduct CCT is about 5 kJ/mol (See Section "Quantum chemical calculations" for further details). At the CoIn, the quantum yields indicate that about 60% of the molecules reach the S_0* state and form the TCT configuration, while 40% relax back to the ground state of TTT.

This relaxation by cooling back to the TTT and gradual recovery of the GSB (400 nm) is described by the third lifetime τ_3 (DAS, green spectra). The cooling process within 24 ps is only evident in MeCN by the blue shift of the spectrum, while in EtOH only the initial recovery of the GSB (84 ps) is visible. Photoproduct absorption (PA) of CCT up to 400 nm is not visible since the negative contribution dominates.

CCT→TTT photoisomerization

The CCT→TTT photoisomerization (Figure 4) shows six contributions (Figure 4) – two negative signals assigned to SE bands at 350 nm and 580 nm, two ESA contributions (ESA1 and ESA2) and two additional positive signatures, one at ~10 ps (CTT) and a final positive band at 400 nm representing the photoproduct (TTT). In contrast to TTT→CCT, five lifetime components had to be applied to obtain an adequate fit. Upon excitation of CCT, the initially populated ESA1 (470 nm) and SE1 (350 nm) decay within 200 fs in both solvents is described by the positive and negative amplitudes in the DAS (Figures 4b and d).

As mentioned above, specific excitation of the CCT isomer is not possible due to the broad spectral overlap of the TTT and CCT absorption bands (Figure 2). Therefore, mixed dynamics of both ground state isomers is observed, that is, the dynamics of the TTT→CCT reaction is also evident in this measurement. After direct excitation, both ESA1, ESA2, SE1 and SE2 are present, confirming the simultaneous excitation of both isomers. Compared to the TTT→CCT isomerization, the TTT isomer exhibits the same dynamics as before (Figure 3). The SE2 signature and the ESA2 band decay simultaneously with the same lifetime τ_2 (DAS, yellow spectra). The decay of the excited TTT-MC is followed by the formation of a positive broad band at 400 nm. As in the previous fs measurements, the CCT→TTT photoreaction after passing the CoIn proceeds via a hot ground state (30% Φ) accompanied by the formation of a transoid MC (CTT) with a ground state barrier of ~15 kJ/mol to the TTT form (see Section "Quantum chemical calculations" for further details). The negative amplitude at 480 nm (DAS) implies the formation of this hot ground state isomer which undergoes an additional isomerization of $>$600 ps towards the ground state equilibrium and is reflected in the negative amplitude at 420 nm. The remaining positive amplitude at 400 nm (τ_{inf}) demonstrates the formation of the photoproduct TTT. Since triplet states are primarily observed in the ring-opening reaction from SP to MC[12,36,37] and these are sometimes expressed in several positive contributions up to the µs time range which are not observed here, it is assumed that no triplet states are involved.

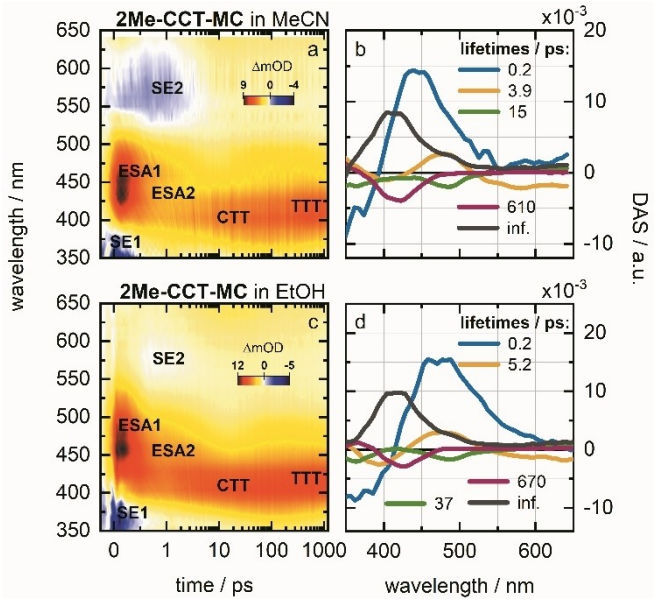

Figure 4. Transient absorption maps of **2Me**-CCT-**MC** in MeCN (a, b) and EtOH (c, d) after excitation with 300 nm with corresponding DAS (b, d). The negative absorption difference signals (dark to light blue) represent stimulated emission (SE) and a ground-state bleach (GSB), as well as a positive difference signal (yellow up to dark red) is either excited state absorption (ESA) or photoproduct absorption (CTT or TTT).

Quantum chemical calculations

Complementary to the time-resolved spectroscopy measurements, ground- and excited state electronic structure calculations were carried out to characterize the photochemical pathways. The relative ground state energies of each of the isomers are shown in Table 2. These were computed using density functional theory (DFT) with the ωB97XD functional[38,39] (as previously used by the authors to study MC-SP

Table 2. Relative ground state energies (kJ mol^{-1}) and dihedral angles α, β and γ (°) of the eight **2MeMC** isomers, computed by ωB97XD/def2TZVP/PCM(MeCN).

Isomer	S_0 Energy (kJ·mol^{-1})	α	β	γ
TTT	0	178	180	189
TTC	0.22	179	180	358
CTC	3.11	36	176	6
CTT	3.73	32	177	192
CCT	7.15	50	6	222
CCC	7.67	47	2	31
TCC	16.7	241	5	31
TCT	16.1	251	7	226

photoisomerization[40]), def2TZVP[41,42] basis set, and MeCN solvent treated with the Polarizable Continuum Model (PCM)[43] in Gaussian 16.[44] The α, β and γ dihedrals are also given, with the *transoid* isomers being mostly planar, while the *cisoid* isomers reveal some deviation from planarity in the α and γ dihedrals. Similar energies and dihedral angles were also found in ethanol solvent (Table S1).

The TTT isomer is calculated to be the most stable *transoid* isomer (and most stable overall), and CCT is the most stable *cisoid* isomer, as well as NMR studies (Figure S6) showing that only TTT was present at the beginning of the measurements in contrast to previous NMR studies on merocyanine indicating a mixture of TTT and TTC.[45–47]

However, we also identified a second potential pathway involving the TTC and CCC isomers, which we cannot completely rule out because of their similarity in energy to TTT and CCT. This pathway is illustrated in the SI. For the remainder of the manuscript we will discuss only the pathway involving TTT and CCT.

Relaxed one-dimensional ground state scans around the α, β and γ dihedral angles starting at the TTT and CCT ground state geometries (see Figures S7 and S8) revealed large barriers (>100 kJ/mol) around the β dihedral, with much smaller barriers (<25 kJ/mol for TTT, <60 kJ/mol for CCT) around the α and γ dihedrals. Conversely, relaxed excited state scans around these dihedrals with time-dependent density functional theory (TD-DFT) (see Figures S9 and S10) revealed significant barriers (>80 kJ/mol for TTT, >50 kJ/mol for CCT) around the α and γ dihedrals, while there were modest barriers around the β dihedral (~10 kJ/mol for TTT, ~20 kJ/mol for CCT), followed by an energetically downhill pathway. Both of these factors are concomitant with a single-double-single bond pattern in the ground state, and double-single-double bond pattern in the excited state. The scan around the β dihedral in the excited state also revealed the close proximity of the ground state at values of β~90° and β~270° for both isomers, indicating the presence of a nearby CoIn.

These CoIns were computed by the complete active space self-consistent field method (CASSCF) method, using an active space of 8 electrons in 8 orbitals, and state averaging over the S_0 and S_1 states. The computed intersections are shown in Figure 5, revealing a peaked and bifurcated nature, both visually and via the numerical analysis implemented in OpenMolcas v22.06.[48–50] This numerical analysis (see Eq. 57 in Ref. [45]) yields parameters P = 0.14 for TTT and P = 0.002 for CCT, indicating the significantly peaked nature of the CoIns, with P < 1 in general indicating a peaked CoIn. They will therefore be efficient funnels for photoproducts in the reactant and product channels, as indicated by the experimental measurements in the previous sections. The degeneracy at the CoIn is lifted in two dimensions, known as the branching space. These directions correspond to the gradient difference vector (denoted $\hat{x}$ in Figure 5) and the nonadiabatic coupling vector (denoted $\hat{y}$ in Figure 5).

For both the TTT and CCT isomers, these directions correspond to a bond-length alternation coordinate of the three central bonds ($\hat{x}$), and a dihedral angle rotation around β ($\hat{y}$). This branching space characterization is similar to that of the archetypal photoisomerization molecule, the protonated Schiff base.[51] Both isomers have a β dihedral of close to 90° at the CoIn, in accordance with the results of the TD-DFT calculations. The α and γ dihedrals for the TTT isomer are similar to the values at the ground state minimum shown in Table 2. The α and γ dihedrals for the CCT isomer display more pronounced changes, however at the CoIn they now more closely resemble "ideal" values of 0° and 180° for *cis* and *trans* dihedrals than in the ground state minimum shown in Table 2. Therefore, for both TTT and CCT, there is no change of isomer label for the α and γ dihedrals in the excited state.

As indicated in the spectroscopy measurements, after passing through the CoIn, a hot ground state species is formed,

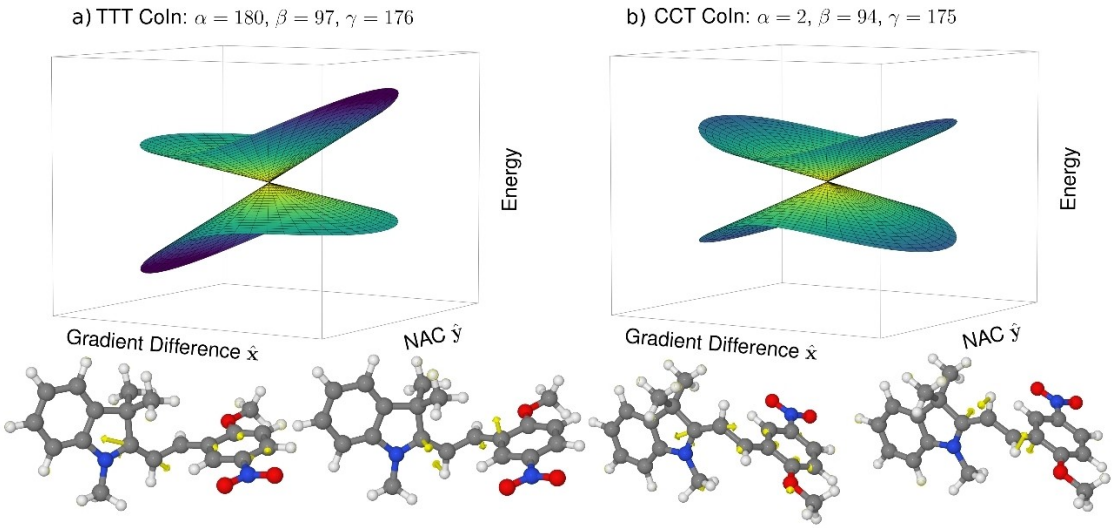

Figure 5. S_1/S_0 conical intersection topologies of the a) TTT and b) CCT isomers computed by SA2-CASSCF (8,8), with dihedrals angles labelled, and the branching plane vectors (gradient difference and non-adiabatic coupling) illustrated.

which then interconverts into the final isomer. In Figure 6 we attempt to map this interconversion process through computation of 3-dimensional cuts through the relaxed ground state potential energy surface, as a function of the α, β and γ dihedrals. Each panel corresponds to a value of β in the range 0–180° in increments of 30°, with the *cisoid* angles appearing on the top row, the *transoid* angles appearing on the bottom row, and β = 90° appearing in the centre. The α and γ dependence for each value of β is displayed in the range 0°–360°, and was computed in increments of 15°. We hypothesize that following passage through the CoIn, the ground state surface would resemble that in the central β = 90° panel, before relaxation in the *cisoid* or *transoid* directions.

For the TTT isomer, after photoexcitation and passage through CoIn, a hot ground state species is produced (denoted TTT* in the central panel of the Figure), with β = 90° and α, γ = 180°, i.e., approximately the same values as those shown in Figure 5. There are significant (> 70 kJ/mol) barriers around the α and γ dihedrals, indicating that immediate relaxation in these directions is unlikely. Following relaxation to the *cisoid* TCT isomer in the β direction, a metastable minimum is observed in the β = 60° and β = 30° panels, with an increase in the α dihedral. Finally, in the β = 0° panel, a lower energy minimum can be observed corresponding to the CCT isomer, with only a 5 kJ/mol barrier from the TCT isomer.

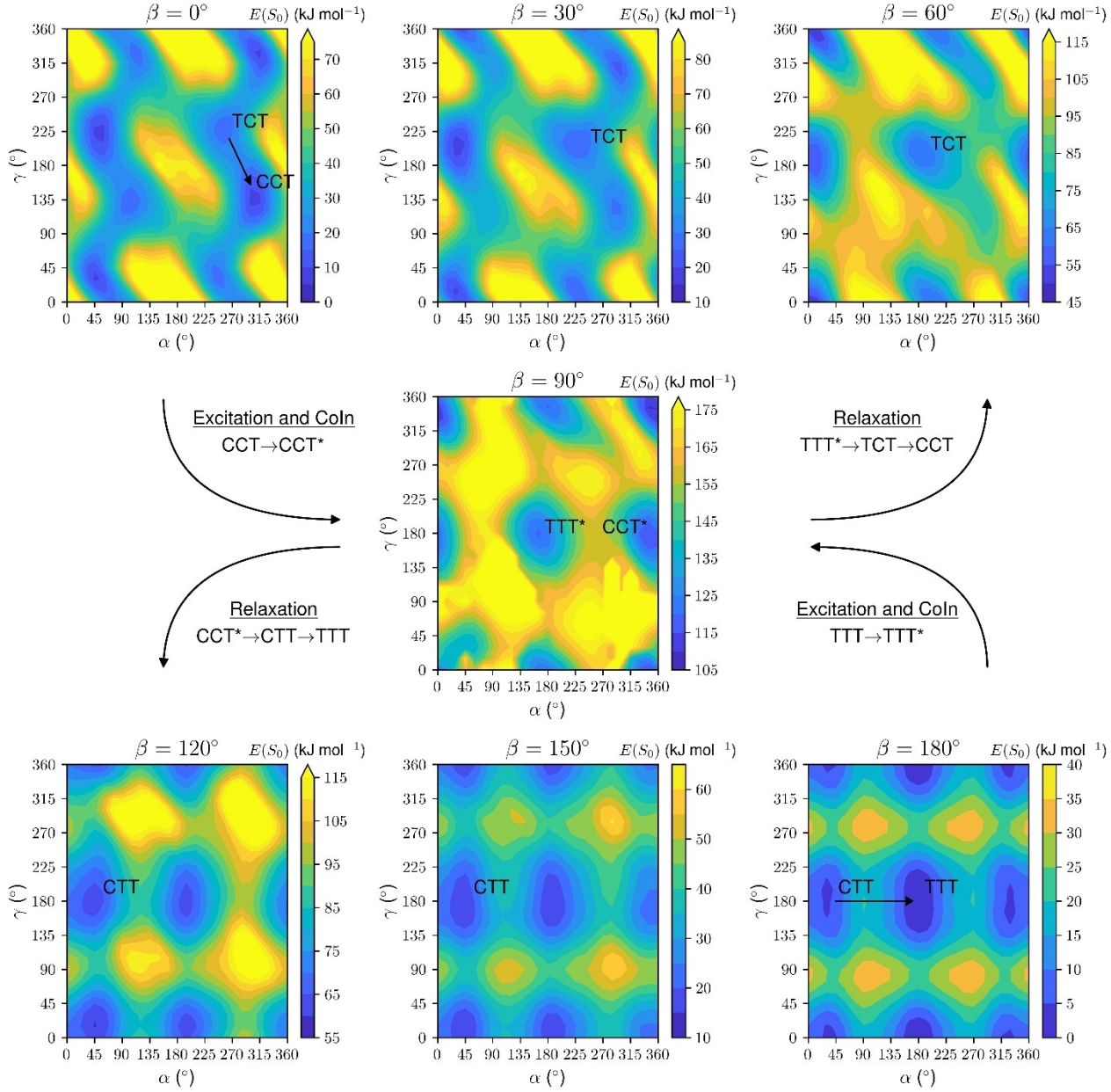

Figure 6. Contour plots of the relaxed ground state potential energy surface for **2MeMC**, as a function of the dihedral angles α, β and γ. Each panel illustrates the α and γ dependence for a particular value of β. Energies relative to the ground state minimum of the TTT isomer. Computed by ωB97XD/def**2**TZVP/PCM(MeCN). Hypothesized photochemical pathway is highlighted, see text for further details.

For the CCT isomer, after photoexcitation and passage through the CoIn, a similar hot ground state species may be produced (denoted CCT* in the central panel of Figure 6), with $\beta = 90°$, $\alpha \sim 360°$ and $\gamma \sim 180°$. These values, like for the TTT* intermediate, resemble the values in Figure 5. Also, similarly to the TTT* intermediate, there are significant (>70 kJ/mol) barriers around these α and γ dihedrals. Relaxation on the *transoid* side to the CTT isomer in the $\beta = 120°$ and $\beta = 150°$ panels illustrates that these barriers subsequently decrease in energy. Finally, in the $\beta = 180°$ panel the barrier in the α direction is the smallest (~15 kJ/mol) and the CTT isomer can inter-convert to the lower energy TTT isomer. A summary of these interconversion pathways is shown in Figure 7.

We hypothesize that the thermal CCT-TTT isomerization pathway proceeds in the reverse direction of the relaxation on the *cisoid* side, i.e., CCT→CTT→TTT. We note that the ground state energies in the $\beta = 90°$ panel relative to those in the $\beta = 0°$ panel could indicate an overestimation of the activation energy compared to the experimental measurement. This would not be completely surprising given the challenging nature of barrier height computations for DFT, even with recent extensive benchmark studies showing that the ωB97XD functional is one of the better performing ones for such calculations.[52]

On the other hand, the activation energy could be affected by local minima along the β dihedral. For example, the structure at (α, β, γ) = (180°, 60°, 195°) corresponds to a local minimum, verified by a lack of imaginary vibrational frequencies. The presence of such local minima could therefore be indicative of a multi-step process along β for the thermal isomerization.

Another possible reason for the overestimation of the activation energy is the lack of explicit solute-solvent interactions in the continuum solvent model.

Conclusions

In summary, we characterized in detail an MC derivative which is non-zwitterionic by simple methylation at its phenolate oxygen and its modification inhibits the ring closure reaction to SP.

A similar effect was found, e.g. for chelating ligands.[53] **2MeMC** proved to be an excellent photoswitch due to its high QYs, especially TTT→CCT ($\Phi_{TTT\rightarrow CCT} = \sim 63\%$, $\Phi_{CCT\rightarrow TTT} = \sim 28\%$), its efficient photoconversions of ~82% for PSS_{420nm} and ~54% (PSS_{300nm}), and its high photostability, especially in H_2O/EtOH. The kinetic parameters also show that the stability of **2MeMC** increases with the proticity of the solvent and that the typically occurring hydrolysis is not observed below 45 °C. Furthermore, the stabilization of **2MeMC** in H_2O/EtOH seems to be caused by the interaction of stronger H-bonds of water. The combination of theoretical calculations and time-resolved absorption measurements indicate for both isomerization mechanisms there is an initiation by a rotation of only the central β dihedral in the excited state (TTT-TCT and CCT-CTT), via a CoIn to the ground state, and which is followed by rotation of the α and γ dihedrals to the thermodynamically more stable isomer (TCT-CCT and CTT-TTT).

Our work provides important insights into the photoisomerization mechanisms of **2MeMC**, which may also be relevant for zwitterionic MCs and SP→MC reactions. With suitable substitution patterns, the merocyanine scaffold offers remarkable flexibility in function, that directly relates to its excited state and ground state topology. Finally, we establish a non-zwitterionic MC photoswitch with excellent switching properties, especially in protic solvents.

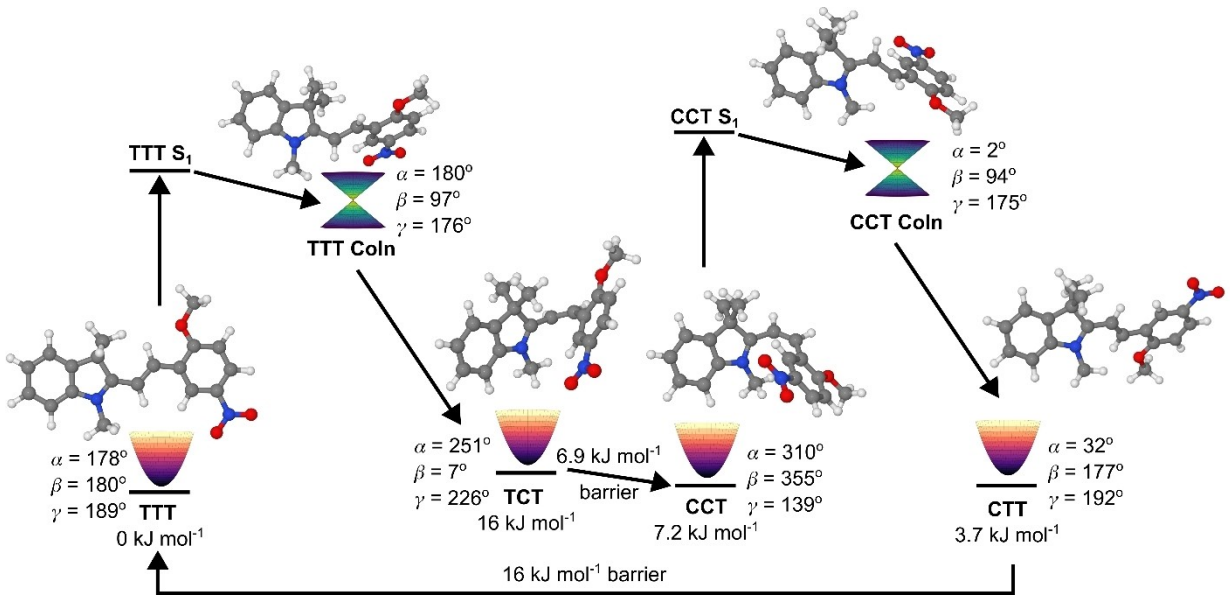

Figure 7. Schematic reaction scheme for the TTT→TCT→CCT and CCT→CTT→TTT photoisomerization cycle, illustrating relevant minima, conical intersections and dihedral angles of the three central bonds of **2MeMC**. Ground state energies relative to the TTT isomer, as well as barriers between the ground state isomers are shown, calculated at the ωB97XD/def2TZVP/PCM(MeCN) level.

Supporting Information

The authors have cited additional references within the Supporting Information (Ref. [35,38,39,43,44,48,49]).

Acknowledgements

J.A.G. gratefully acknowledges funding of a research fellowship by the Alexander von Humboldt foundation. J.W., N.B., M.B. and C.K. appreciate funding by the Deutsche Forschungsgemeinschaft (WA 1850/4-3) and SFB902 "Molecular Principles of RNA-based Regulation", as well as CLiC (Complex Light Control, GRK 1986). C.B.M. acknowledges Carl Tryggers Foundation for the Postdoctoral fellowship.

We thank Gabriele Sentis for her help with NMR measurements and data evaluation. Open Access funding enabled and organized by Projekt DEAL.

Conflict of Interests

The authors declare no conflict of interest.

Data Availability Statement

The data that support the findings of this study are available from the corresponding author upon reasonable request.

Keywords: isomerization pathways · merocyanine · photoswitches · quantum chemistry · time-resolved spectroscopy

[1] Y. Zhao, S. Ippolito, P. Samorì, *Adv. Opt. Mater.* **2019**, *7*, 1–25.
[2] M. Hauck, M. Stolte, J. Schönhaber, H.-G. Kuball, T. J. J. Müller, *Chem. Eur. J.* **2011**, *17*, 9984–9998.
[3] M. M. Lerch, M. J. Hansen, G. M. van Dam, W. Szymanski, B. L. Feringa, *Angew. Chem. Int. Ed.* **2016**, *55*, 10978–10999.
[4] W. Szymanski, J. M. Beierle, H. A. V. Kistemaker, W. A. Velema, B. L. Feringa, *Chem. Rev.* **2013**, *113*, 6114–6178.
[5] F. Würthner, R. Wortmann, K. Meerholz, *ChemPhysChem* **2002**, *3*, 17–31.
[6] H. M. D. Bandara, S. C. Burdette, *Chem. Soc. Rev.* **2012**, *41*, 1809–1825.
[7] A. A. Beharry, G. A. Woolley, *Chem. Soc. Rev.* **2011**, *40*, 4422.
[8] O. Babii, S. Afonin, M. Berditsch, S. Reiβer, P. K. Mykhailiuk, V. S. Kubyshkin, T. Steinbrecher, A. S. Ulrich, I. V Komarov, *Angew. Chem. Int. Ed.* **2014**, *53*, 3392–3395.
[9] D. Lachmann, R. Lahmy, B. König, *Eur. J. Org. Chem.* **2019**, *2019*, 5018–5024.
[10] F. Wilkinson, D. A. Reeves, *J. Chem. Soc. Faraday Trans. 2* **1973**, *69*, 1381–1390.
[11] L. Kortekaas, W. R. Browne, *Chem. Soc. Rev.* **2019**, *48*, 3406–3424.
[12] C. Kaiser, T. Halbritter, A. Heckel, J. Wachtveitl, *ChemistrySelect* **2017**, *2*, 4111–4123.
[13] H. M. D. Bandara, S. C. Burdette, *Chem. Soc. Rev.* **2012**, *41*, 1809–1825.
[14] H. B. Cheng, S. Zhang, J. Qi, X. J. Liang, J. Yoon, *Adv. Mater.* **2021**, *33*, 1–42.
[15] C. Slavov, C. Yang, A. H. Heindl, H. A. Wegner, A. Dreuw, J. Wachtveitl, *Angew. Chem. Int. Ed.* **2020**, *59*, 380–387.
[16] C. Slavov, C. Yang, L. Schweighauser, C. Boumrifak, A. Dreuw, H. A. Wegner, J. Wachtveitl, *Phys. Chem. Chem. Phys.* **2016**, *18*, 14795–14804.
[17] Y. Yokoyama, *Chem. Rev.* **2000**, *100*, 1717–1739.
[18] S. Draxler, T. Brust, S. Malkmus, J. A. DiGirolamo, W. J. Lees, W. Zinth, M. Braun, *Physical chemistry chemical physics: PCCP* **2009**, *11*, 5019–5027.
[19] B. Mravec, J. Filo, K. Csicsai, V. Garaj, M. Kemka, A. Marini, M. Mantero, A. Bianco, M. Cigáň, *Phys. Chem. Chem. Phys.* **2019**, *21*, 24749–24757.
[20] H. Qian, S. Pramanik, I. Aprahamian, *J. Am. Chem. Soc.* **2017**, *139*, 9140–9143.
[21] N. P. Ernsting, T. Arthen-Engeland, *J. Phys. Chem.* **1991**, *95*, 5502–5509.
[22] S. Ruetzel, M. Diekmann, P. Nuernberger, C. Walter, B. Engels, T. Brixner, *Journal of Chemical Physics* **2014**, *140*, 1–10 DOI 10.1063/1.4881258.
[23] L. Kortekaas, J. Chen, D. Jacquemin, W. R. Browne, *J. Phys. Chem. B* **2018**, *122*, 6423–6430.
[24] J. Buback, P. Nuernberger, M. Kullmann, F. Langhojer, R. Schmidt, F. Würthner, T. Brixner, *J. Phys. Chem. A* **2011**, *115*, 3924–3935.
[25] C. Walter, S. Ruetzel, M. Diekmann, P. Nuernberger, T. Brixner, B. Engels, *Journal of Chemical Physics* **2014**, *140*, 1–9 DOI 10.1063/1.4881259.
[26] M. Kullmann, S. Ruetzel, J. Buback, P. Nuernberger, T. Brixner, *J. Am. Chem. Soc.* **2011**, *133*, 13074–13080.
[27] C. M. Nunes, N. A. M. Pereira, R. Fausto, *J. Phys. Chem. A* **2022**, *126*, 2222–2233.
[28] Y. Futami, M. L. S. Chin, S. Kudoh, M. Takayanagi, M. Nakata, *Chem. Phys. Lett.* **2003**, *370*, 460–468.
[29] C. L. Fleming, S. Li, M. Grøtli, J. Andréasson, *J. Am. Chem. Soc.* **2018**, *140*, 14069–14072.
[30] C. Özçoban, T. Halbritter, S. Steinwand, L.-M. Herzig, J. Kohl-Landgraf, N. Askari, F. Groher, B. Fürtig, C. Richter, H. Schwalbe, B. Suess, J. Wachtveitl, A. Heckel, *Org. Lett.* **2015**, *17*, 1517–1520.
[31] M. Hammarson, J. R. Nilsson, S. Li, T. Beke-Somfai, J. Andréasson, *J. Phys. Chem. B* **2013**, *117*, 13561–13571.
[32] J. Sunamoto, K. Iwamoto, M. Akutagawa, M. Nagase, H. Kondo, *J. Am. Chem. Soc.* **1982**, *104*, 4904–4907.
[33] Y. Shiraishi, M. Itoh, T. Hirai, *Phys. Chem. Chem. Phys.* **2010**, *12*, 13737–13745.
[34] L. Wu, Y. Dai, X. Jiang, C. Petchprayoon, J. E. Lee, T. Jiang, Y. Yan, G. Marriott, *PLoS One* **2013**, *8*, 6–13.
[35] C. Slavov, H. Hartmann, J. Wachtveitl, *Anal. Chem.* **2015**, *87*, 2328–2336.
[36] H. Görner, *Phys. Chem. Chem. Phys.* **2001**, *3*, 416–423.
[37] A. K. Chibisov, H. Görner, *J. Phys. Chem.* **1997**, *101*, 4305–4312.
[38] J.-D. Chai, M. Head-Gordon, *J. Chem. Phys.* **2008**, *128*, 084106.
[39] J.-D. Chai, M. Head-Gordon, *Phys. Chem. Chem. Phys.* **2008**, *10*, 6615.
[40] S. Prager, I. Burghardt, A. Dreuw, *J. Phys. Chem. A* **2014**, *118*, 1339–1349.
[41] F. Weigend, R. Ahlrichs, *Phys. Chem. Chem. Phys.* **2005**, *7*, 3297.
[42] F. Weigend, *Phys. Chem. Chem. Phys.* **2006**, *8*, 1057.
[43] J. Tomasi, B. Mennucci, R. Cammi, *Chem. Rev.* **2005**, *105*, 2999–3094.
[44] M. J. Frisch, G. W. Trucks, H. B. Schlegel, G. E. Scuseria, M. A. Robb, J. R. Cheeseman, G. Scalmani, V. Barone, G. A. Petersson, H. Nakatsuji, X. Li, M. Caricato, A. V. Marenich, J. Bloino, B. G. Janesko, R. Gomperts, B. Mennucci, H. P. Hratchian, J. V. Ortiz, A. F. Izmaylov, J. L. Sonnenberg, Williams, F. Ding, F. Lipparini, F. Egidi, J. Goings, B. Peng, A. Petrone, T. Henderson, D. Ranasinghe, V. G. Zakrzewski, J. Gao, N. Rega, G. Zheng, W. Liang, M. Hada, M. Ehara, K. Toyota, R. Fukuda, J. Hasegawa, M. Ishida, T. Nakajima, Y. Honda, O. Kitao, H. Nakai, T. Vreven, K. Throssell, J. A. Montgomery Jr., J. E. Peralta, F. Ogliaro, M. J. Bearpark, J. J. Heyd, E. N. Brothers, K. N. Kudin, V. N. Staroverov, T. A. Keith, R. Kobayashi, J. Normand, K. Raghavachari, A. P. Rendell, J. C. Burant, S. S. Iyengar, J. Tomasi, M. Cossi, J. M. Millam, M. Klene, C. Adamo, R. Cammi, J. W. Ochterski, R. L. Martin, K. Morokuma, O. Farkas, J. B. Foresman, D. J. Fox, Gaussian 16, revision B.01; Gaussian Inc.: Wallingford, CT, **2016**.
[45] J. Hobley, *Phys. Chem. Chem. Phys.* **2000**, *2*, 53–56.
[46] J. Hobley, V. Malatesta, *Phys. Chem. Chem. Phys.* **2000**, *2*, 57–59.
[47] J. Hobley, V. Malatesta, R. Millini, W. O. N. Parker, *Phys. Chem. Chem. Phys.* **1999**, *1*, 3259–3267.
[48] I. Fdez, Galván, M. Vacher, A. Alavi, C. Angeli, F. Aquilante, J. Autschbach, J. J. Bao, S. I. Bokarev, N. A. Bogdanov, R. K. Carlson, L. F. Chibotaru, J. Creutzberg, N. Dattani, M. G. Delcey, S. S. Dong, A. Dreuw, L. Freitag, L. M. Frutos, L. Gagliardi, F. Gendron, A. Giussani, L. González, G. Grell, M. Guo, C. E. Hoyer, M. Johansson, S. Keller, S. Knecht, G. Kovačević, E. Källman, G. Li Manni, M. Lundberg, Y. Ma, S. Mai, J. P. Malhado, P. Å. Malmqvist, P. Marquetand, S. A. Mewes, J. Norell, M. Olivucci, M. Oppel, Q. M. Phung, K. Pierloot, F. Plasser, M. Reiher, A. M. Sand, I. Schapiro, P. Sharma, C. J. Stein, L. K. Sørensen, D. G. Truhlar, M. Ugandi, L. Ungur, A. Valentini, S. Vancoillie, V. Veryazov, O. Weser, T. A. Wesołowski, P.-O. Widmark, S. Wouters, A. Zech, J. P. Zobel, R. Lindh, *J. Chem. Theory Comput.* **2019**, *15*, 5925–5964.
[49] F. Aquilante, J. Autschbach, A. Baiardi, S. Battaglia, V. A. Borin, L. F. Chibotaru, I. Conti, L. De Vico, M. Delcey, I. Fdez, Galván, N. Ferré, L.

Freitag, M. Garavelli, X. Gong, S. Knecht, E. D. Larsson, R. Lindh, M. Lundberg, P. Å. Malmqvist, A. Nenov, J. Norell, M. Odelius, M. Olivucci, T. B. Pedersen, L. Pedraza-González, Q. M. Phung, K. Pierloot, M. Reiher, I. Schapiro, J. Segarra-Martí, F. Segatta, L. Seijo, S. Sen, D.-C. Sergentu, C. J. Stein, L. Ungur, M. Vacher, A. Valentini, V. Veryazov, *J. Chem. Phys.* **2020**, *152*, 214117.
[50] I. Fdez, Galván, M. G. Delcey, T. B. Pedersen, F. Aquilante, R. Lindh, *J. Chem. Theory Comput.* **2016**, *12*, 3636–3653.
[51] M. Garavelli, P. Celani, F. Bernardi, M. A. Robb, M. Olivucci, *J. Am. Chem. Soc.* **1997**, *119*, 6891–6901.
[52] N. Mardirossian, M. Head-Gordon, *Mol. Phys.* **2017**, *115*, 2315–2372.
[53] P. Selvanathan, V. Dorcet, T. Roisnel, K. Bernot, G. Huang, B. Le Guennic, L. Norel, S. Rigaut, *Dalton Trans.* **2018**, *47*, 4139–4148.

Manuscript received: December 14, 2023
Revised manuscript received: January 17, 2024
Accepted manuscript online: January 19, 2024
Version of record online: February 2, 2024

RESEARCH ARTICLE

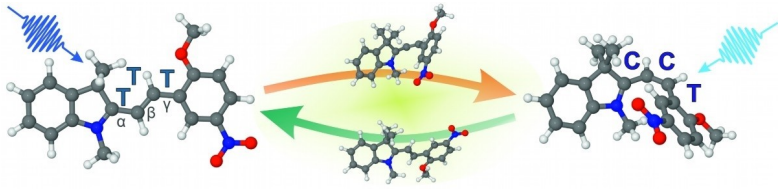

The non-zwitterionic merocyanine derivative **2MeMC** is a photoswitch with outstanding photoisomerization efficiency, photostability, especially in protic environment, and high switching rates, whose ring closure reaction to the spiropyran is inhibited by methylation of the phenolate oxygen. Ultrafast spectroscopy and quantum chemical calculations reveal the photoisomerization mechanism of this *trans*(TTT)-*cis* (CCT)-only merocyanine.

N. Blaise, Dr. J. A. Green, Dr. C. Benitez-Martin, Dr. C. Kaiser, Dr. M. Braun, J. M. Schaible, Prof. J. Andréasson, Prof. I. Burghardt, Prof. J. Wachtveitl**

1 – 10

Isomerization dynamics of a novel *cis/trans*-only merocyanine